The effects of orientation and attention during surround suppression of small image features: A 7 Tesla fMRI study

Michael-Paul Schallmo Graduate Program in Neuroscience, University of Minnesota, Minneapolis, MN, USA

Andrea N. Grant Department of Neuroscience, University of Minnesota, Minneapolis, MN, USA

Philip C. Burton Office of the Associate Dean for Research, University of Minnesota, Minneapolis, MN, USA

Cheryl A. Olman Department of Psychology, University of Minnesota, Minneapolis, MN, USA

Although V1 responses are driven primarily by elements within a neuron's receptive field, which subtends about 1° visual angle in parafoveal regions, previous work has shown that localized fMRI responses to visual elements reflect not only local feature encoding but also long-range pattern attributes. However, separating the response to an image feature from the response to the surrounding stimulus and studying the interactions between these two responses demands both spatial precision and signal independence, which may be challenging to attain with fMRI. The present study used 7 Tesla fMRI with 1.2-mm resolution to measure the interactions between small sinusoidal grating patches (targets) at 3° eccentricity and surrounds of various sizes and orientations to test the conditions under which localized, context-dependent fMRI responses could be predicted from either psychophysical or electrophysiological data. Targets were presented at 8%, 16%, and 32% contrast while manipulating (a) spatial extent of parallel (strongly suppressive) or orthogonal (weakly suppressive) surrounds, (b) locus of attention, (c) stimulus onset asynchrony between target and surround, and (d) blocked versus event-related design. In all experiments, the V1 fMRI signal was lower when target stimuli were flanked by parallel versus orthogonal context. Attention amplified fMRI responses to all stimuli but did not show a selective effect on central target responses or a measurable effect on orientation-dependent surround suppression. Suppression of the V1 fMRI response by parallel surrounds was stronger than predicted from psychophysics but showed a better match to previous electrophysiological reports.

Introduction

A direct, quantitative relationship between functional MRI activity in primary visual cortex (V1) and the luminance contrast of an isolated stimulus is well established (Boynton, Demb, Glover, & Heeger, 1999; Boynton, Engel, Glover, & Heeger, 1996; Heeger, Huk, Geisler, & Albrecht, 2000; Olman, Ugurbil, Schrater, & Kersten, 2004; Schumacher, Thompson, & Olman, 2011). However, understanding how V1 also encodes interactions between neighboring stimuli (contextual modulation) has proved more challenging. A well-studied example of contextual modulation in V1 is orientation-dependent surround suppression (ODSS): A neuron's response to a stimulus in its classical receptive field is typically suppressed by simultaneous presentation of surrounding stimuli, and this suppression is greater when the surround is similar (e.g., parallel) to the center (Cavanaugh, Bair, & Movshon, 2002; DeAngelis, Freeman, & Ohzawa, 1994; Henry, Joshi, Xing, Shapley, & Hawken, 2013; Levitt & Lund, 1997; Shushruth et al., 2013; Walker, Ohzawa, & Freeman, 1999; Webb, Dhruv, Solomon, Tailby, & Lennie, 2005). However, the V1 fMRI response to small image features (i.e., small gratings or Gabors) presented with flanking stimuli (Joo, Boynton, & Murray, 2012; Schumacher & Olman, 2010) does not

Citation: Schallmo, M.-P., Grant, A. N., Burton, P. C., & Olman, C. A. (2016). The effects of orientation and attention during surround suppression of small image features: A 7 Tesla fMRI study. *Journal of Vision*, *16*(10):19, 1–21, doi:10.1167/16.10.19.

doi: 10.1167/16.10.19 Received May 7, 2016; published August 26, 2016 ISSN 1534-7362

always reflect the straightforward ODSS that is observed for configurations of larger stimuli (Chen, 2014; McDonald, Seymore, Schira, Spehar, & Clifford, 2009; Nurminen, Kilpelainen, Laurinen, & Vanni, 2009; Nurminen, Kilpelainen, & Vanni, 2013; Pihlaja, Henriksson, James, & Vanni, 2008; Williams, Singh, & Smith, 2003; Zenger-Landolt & Heeger, 2003).

It is also well established that isolated stimuli evoke stronger V1 fMRI responses when attended than when ignored (Bouvier & Engel, 2011; Brefczynski & DeYoe, 1999; Bressler, Fortenbaugh, Robertson, & Silver, 2013; Buracas & Boynton, 2007; Kastner, de Weerd, Desimone, & Ungerleider, 1998; Li, Lu, Tjan, Dosher, & Chu, 2008; Murray, 2008; Tootell et al., 1998). This literature suggests that across target contrast levels, the effects of attention in V1 may be characterized by a baseline offset (i.e., increasing the *y*-intercept of the contrast-response function; Buracas & Boynton, 2007; Li et al., 2008; Murray, 2008). Attention also modulates center–surround interactions (Flevaris & Murray, 2015; Müller & Kleinschmidt, 2004; Sanayei, Herrero, Distler, & Thiele, 2015), but it is not yet clear how attention may affect contrast–response relationships during surround suppression.

The single-unit electrophysiology literature provides good estimates of contrast response functions for a wide range of target and surround stimuli in *anesthetized* nonhuman primates (Cavanaugh et al., 2002; Henry et al., 2013; Shen, Xu, & Li, 2007). However, because of the difficulty of studying surround suppression in awake animals (in which small eye movements may confound responses), limited data are available to characterize contextual modulation of *attended* stimuli (Pooresmaeili, Poort, Thiele, & Roelfsema, 2010; Sanayei et al., 2015), and contrast response functions for attended targets and surrounds have not been measured. Therefore, psychophysical data currently provide most of our estimates of surround suppression for attended stimuli (Cannon & Fullenkamp, 1991; Petrov & McKee, 2006; Schallmo & Murray, 2016; Snowden & Hammett, 1998; Tadin, Lappin, Gilroy, & Blake, 2003; Xing & Heeger, 2000; Yu, Klein, & Levi, 2001, 2003; Zenger, Braun, & Koch, 2000). The experiments in this study were intended to fill this gap by determining whether fMRI can accurately characterize contextual modulation of neuronal responses to small image features under a variety of conditions. To this end, a series of five experiments characterized the magnitude of the fMRI response as a function of stimulus contrast while varying the relative size and orientation of surrounding features, both with and without attention directed at the stimuli.

This study additionally explores the methodological challenges unique to studying individual image features embedded in a surrounding context. Two primary methodological factors complicate the use of fMRI to quantify surround suppression of small image features: neural signal overlap (Olman, Inati, & Heeger, 2007; Pihlaja et al., 2008) and potential nonlinearities in the hemodynamic response (Bao, Purington, & Tjan, 2015). Considering signal overlap: Although the early fMRI literature was dominated by concerns about hemodynamic blurring (e.g., "water the entire garden for the sake of one thirsty flower"; Malonek & Grinvald, 1996), many recent studies show that the fMRI signal can be selective at the submillimeter level with appropriate experiment design and acquisition strategies (Cheng, Wagooner, & Tanaka, 2001; Kok, Bains, van Mourik, Norris, & de Lange, 2016; Kok & de Lange, 2014; Olman et al., 2012; Olman et al., 2007; Yacoub, Harel, & Ugurbil, 2008). The concern about signal overlap, therefore, is not a matter of hemodynamic blurring. At the spatial scale required to study interactions between small adjacent visual stimuli, neuronal signals themselves may overlap, which presents a problem. If isolation of responses to the target stimuli is impossible, fMRI voxels may contain neurons responding to both target and surround stimuli, and analyses must rely on comparison between surround-alone and surround-plus-target stimuli (Millin, Arman, Chung, & Tjan, 2014; Zenger-Landolt & Heeger, 2003).

Although subtractive analyses may thus be advantageous when studying contextual modulation of small image elements, any nonlinearity in the hemodynamic response will limit the utility of such analyses. If hemodynamic responses are linear, then the surround response can be estimated separately and subtracted out from the target + surround response. However, if the responses to target and surround within a single voxel do not sum linearly, then it becomes difficult to quantify responses unique to the target, and such a nonlinearity may also limit the dynamic range for measuring the responses of interest. This problem is reduced for stimuli with relatively large cortical representations: When there is relatively little overlap between cortical territory stimulated by target and surround, the presence of the surround does not greatly affect the hemodynamic response to the target. Indeed, a quantitative match between fMRI and psychophysical measurements of surround suppression has been established for large annuli (Zenger-Landolt & Heeger, 2003). The present study examined whether quantitative relationships between psychophysical and fMRI data can be drawn for small stimuli as well. A previous attempt with low-resolution imaging showed a mismatch between fMRI and the anticipated neuronal response (Schumacher & Olman, 2010); this study considers whether better signal localization can account for that mismatch.

Methods

Participants

A total of 12 people (four female and eight male, mean age 31 years) participated across five experiments after providing written informed consent. The experimental protocol was approved by the University of Minnesota Institutional Review Board.

Nine subjects participated in each of four experiments (referred to below as the *Attended Disks*, *Attended Gabors*, *Distracted Gabors*, and *Block Gabors* experiments). Seven of those subjects also took part in a fifth experiment (*Distracted Disks*) along with three additional participants (10 subjects total). All subjects had normal or corrected-to-normal vision. Five subjects were experienced psychophysical observers, and four of the subjects were the authors.

Visual display

Stimuli were projected on a screen mounted inside the bore of the magnet using a Sony VPL-PX10 or (following an equipment failure) NEC NP4100 projector and were viewed from a distance of 72 cm through a mirror mounted on the head coil. Mean luminance was 158 cd/m^2 for the original and 79 cd/m^2 for the replacement projector. Display luminance was linearized using custom MATLAB (The Mathworks, Natick, MA) code. Stimuli were generated using PsychToolbox (Brainard, 1997; Pelli, 1997) and MATLAB on a Macintosh running OS X. Subjects made behavioral responses during the scan using a four-button fiber optic response pad (Current Designs, Philadelphia, PA).

Disks stimuli

In the first two experiments (*Attended Disks* and *Distracted Disks*), stimuli consisted of a circular target surrounded in a subset of trials by an annulus (Figure 1A). Targets and surrounds were sinusoidally modulated luminance gratings with a spatial frequency of 3 c/°. This stimulus geometry has been used extensively to investigate the neural and perceptual mechanisms of ODSS (Cavanaugh et al., 2002; Shushruth et al., 2013). Target gratings with a radius of 0.75° were presented simultaneously in all four quadrants of the screen at 3° eccentricity from a central fixation mark (white square, 0.2° diameter). Target stimulus orientation was ±45° from vertical, and thus gratings were aligned in a radial direction with respect to fixation. Surround annuli were 0.75° wide with a 0.375° gap between the outer edge of the target and the inner edge of the surround (i.e., surround annuli had inner and outer radii of 1.125° and 1.875°). Stimulus mask edges were blurred with a Gaussian envelope ($\sigma = 0.094°$). This blurring reduced the 0.375° gap between target and surround to a small gap (approximately 0.1° wide) with average Michelson contrast equal to half that of the target. Targets were presented at 8%, 16%, and 32% contrast in separate conditions. Surrounding annuli were always presented at 50% contrast with an orientation that was either parallel (0°) or orthogonal (90°) to the surrounded target. When

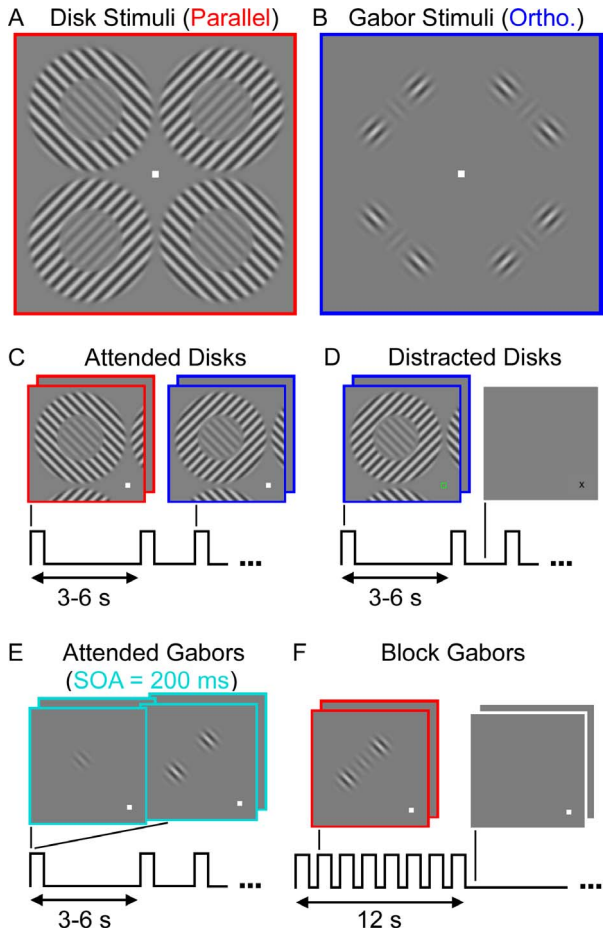

Figure 1. Stimuli and presentation paradigms. (A) *Disks* stimuli. (B) *Gabors* stimuli. (C) Attended event-related paradigm, showing *Disks* stimuli in one quadrant. Two overlapping panels are shown for each example stimulus to illustrate the two stimulus presentation intervals in each trial. The boxcar function at the bottom illustrates the event-related paradigm (trials occurred every 3–6 s). (D) Distracting fixation paradigm. Note the fixation task timing is independent from that of the peripheral gratings (*Disks* shown). (E) An illustration of the 200-ms SOA between targets and surrounds in the *Attended Gabors* experiment. Target and flanking Gabors are shown in separate panels to indicate the asynchrony. (F) Blocked paradigm from the *Block Gabors* experiment with block timing illustrated by the clustered boxcar function (one block comprised eight trials, 1.5 s each).

parallel, targets and surrounds had the same spatial phase.

Gabors stimuli

Stimuli presented in the other three experiments (*Attended Gabors*, *Distracted Gabors*, and *Block Gabors*; Figure 1B) matched those used by Schumacher and Olman (2010). Target stimuli were Gabor elements ($\sigma = 0.25°$; full width at half maximum of 0.6°) with a spatial frequency of 3 c/°. Four target Gabors were presented at 3° eccentricity, one in each visual quadrant, oriented ±45° from vertical, aligned radially toward fixation. In a subset of trials, two flanking Gabors (same spatial frequency and bandwidth) were presented with each target Gabor, positioned 1° (center to center) from the corresponding target along a tangential axis relative to fixation. Flanking Gabors were always presented at 50% contrast with an orientation that was either parallel (0°) or orthogonal (90°) to the flanked target.

Paradigm

Each experiment measured fMRI responses during eight stimulus conditions. All experiments included a Target-Alone condition in which the contrast of the targets was 16% and a Surround-Alone condition with surrounds presented at 50% contrast. The remaining six conditions were combinations of three pedestal contrast levels (8%, 16%, and 32%) and two surround configurations (parallel and orthogonal in the *Disks*, *Block Gabors*, and *Distracted Gabors* experiments; parallel with stimulus-onset asynchrony of 0 ms and 200 ms in the *Attended Gabors* experiment). Subjects were instructed to keep their eyes on the fixation mark at the center of the screen throughout each experiment. Each scanning session for each experiment contained eight fMRI scans: two functional localizers used for region of interest (ROI) definition and six task scans during which the eight experimental conditions were presented.

Attended Disks experiment

During the *Attended Disks* experiment task scans, circular gratings with annular surrounds were presented in an event-related paradigm (Figure 1C) with trial-onset intervals of 3, 4.5, or 6 s (uniformly and randomly distributed). Trials were composed of two 150-ms stimulus presentations (intervals), each followed by a mean luminance background presented for 750 ms. The eight conditions were interleaved randomly with 10 trials for each condition per scan. Task scan duration was 6.25 min. For one subject in this experiment, task scans were longer (299 repetition times [TRs], 7.2 min) with stimuli from each of the eight conditions presented 12 times. In this case, only four task scans were completed.

During the task scans, subjects performed a two-interval forced-choice (2IFC) task, responding to a contrast increment in one of the four target stimuli during one of the two intervals. In order to properly control for the effects of attention, this task was also performed during the Surround-Alone condition in which the target pedestal contrast was 0% (detection). The target quadrant and the interval for which the contrast was augmented were both randomly assigned. For all conditions, the contrast increments varied between trials (starting value 7.3%, range 1.6%–40%) and were determined by independent three-down, one-up staircases, converging on 79% accuracy (Garcia-Perez, 1998) in order to control task difficulty. Feedback was given after each trial for 200 ms with the fixation mark turning green for correct responses or red for incorrect responses.

Because of the small number of trials and the difficulty of performing a rapid discrimination task in the scanner, there was not sufficient behavioral data to measure contrast perception psychophysically during scanning for all subjects. Instead, a subset of subjects returned for a second psychophysical session inside the scanner (see Methods, "Behavioral experiment"). Contrast discrimination thresholds obtained during scanning were higher in the presence of parallel versus orthogonal surrounds or no surround (data not shown), consistent with the full behavioral data sets acquired later. This reflects the expected ODSS during contrast perception within the scanning sessions (Yu et al., 2003). As there were four target positions in each of two stimulus presentation intervals, the true average contrast for each target was larger than the pedestal contrast by approximately one eighth of the threshold contrast increment. Across all the conditions and subjects analyzed, there was an average increase in target contrast of 1.4% in the *Attended Disks* experiment.

Distracted Disks experiment

In the *Distracted Disks* experiment, circular gratings with annular surrounds were presented in an event-related paradigm as in the *Attended Disks* experiment. The structure of the scanning session and the timing of the stimulus presentation within each scan were identical to the *Attended Disks* experiment. In this experiment, subjects were instructed to ignore the disks and instead focus their attention on a demanding reaction time task presented at fixation (Figure 1D). Subjects monitored the central fixation point for the

brief presentation of a black "X"; a full description of this task is given below.

The fixation task used during the *Distracted* experiments was designed to be challenging so that subjects had to focus their attention on the fixation stimuli, thus diverting attention away from the peripheral gratings. The objective of the task was for subjects to press a button before the X disappeared in order to earn or retain points (starting value 10). Prior to presentation of the fixation target, a colored fixation mark cue appeared for a variable duration (1.5 to 3.5 s). Cues indicated both that a target was about to appear and that correct performance during the subsequent fixation trial would allow the subject either to win a single point (green square cue preceding appearance of the X indicated an opportunity to win) or to prevent the loss of a point (red square cue indicated upcoming opportunity to lose). Failing to respond quickly enough on a win trial had no effect on the point total, and failing on a loss trial cost subjects one point. After each fixation trial, feedback was given for 500 ms (X turned green when earning a point, red when losing, and blue for no change), and then the current point total was displayed for 500 ms. Fixation task trials appeared every 5–7 s, and their timing was independent of the stimulus presentation.

Fixation task difficulty was adjusted between scans by shortening the duration for which the X was presented in order to ensure the attentional demands of the task were sufficiently high. The duration of the X at the beginning of a scanning session was 400 ms. If accuracy during the previous scan was greater than 66%, the X stimulus duration was reduced by 50 ms, and if accuracy was less than 33%, the duration was increased by 50 ms. Accuracy was moderate across subjects (mean 64%, *SEM* 7.1%), suggesting they were engaged in the task but not performing at ceiling.

Attended Gabors experiment

In the *Attended Gabors* experiment task scans, target Gabors were presented with parallel flanking Gabors that appeared with a stimulus-onset asynchrony (SOA) of either 0 ms or 200 ms (Figure 1E). Because target duration was 150 ms, targets and parallel flanking Gabors did not appear on the screen at the same time when SOA was 200 ms. The SOA of 200 ms was chosen because it is sufficiently long to minimize orientation-dependent masking by the surround (Ishikawa, Shimegi, & Sato, 2006) but too short to interfere with sluggish hemodynamic effects, such as blood stealing by regions outside the target ROI (Shmuel et al., 2002; A. T. Smith, Williams, & Singh, 2004; Zenger-Landolt & Heeger, 2003). The event-related paradigm matched that of the *Attended Disks* experiment, and subjects again performed a 2IFC contrast discrimination task (i.e., attention directed to the target Gabor stimuli). Data from one task scan in one subject from the *Attended Gabors* experiment were excluded because the scan was terminated early. During scanning, larger contrast increments were observed in this task for the 0-ms SOA compared to the 200-ms SOA condition as would be expected if the 200-ms SOA reduced neural interactions (Ishikawa et al., 2006). On average, target contrast increased by 2.2% due to the 2IFC task.

Distracted Gabors experiment

In the *Distracted Gabors* experiment, Gabor stimuli (eight conditions) were presented in an event-related paradigm matching the *Disks* experiments. Subjects performed the demanding fixation task from the *Distracted Disks* experiment (Figure 1D) in order to divert attention away from the Gabor stimuli. Accuracy on this task (mean 69%, *SEM* 4.0%) was comparable with the *Distracted Disks* experiment.

Block Gabors experiment

During task scans in the *Block Gabors* experiment, the Gabor stimuli (eight conditions) were presented in a mixed block design (Figure 1F). In this experiment, one trial consisted of two 150-ms stimulus presentations with a 500-ms interstimulus interval (a slightly faster pace than event-related design) and a trial onset interval of 1.5 s. Subjects performed the same 2IFC contrast discrimination task as in the event-related design except the feedback duration in this experiment was 100 ms. Stimuli from each condition were grouped in 12-s blocks (eight trials per block) presented in a pseudorandom order with two blocks of each condition presented in every task scan. Each scan began with a 12-s block during which a mean luminance blank screen was presented, and a blank block followed each stimulus block. Blank blocks consisted of eight trials during which no flanking Gabors were present, and the pedestal contrast was 0% while subjects performed a 2IFC contrast detection task. The structure of the blank blocks equated attentional and task demands between blank and stimulus blocks, with the former serving as the response baseline in this experiment. Each task scan in this experiment lasted 6.6 min. Contrast increments in the 2IFC task during scanning tended to be higher for parallel versus orthogonal surrounds as in the *Attended Disks* experiment. This task led to an average increase in target contrast of 2.8%.

Functional localizers

Disks experiments included functional localizer scans in which Target-Alone stimuli alternated with Sur-

Condition	*A*	*p*	*q*	*σ*
Target-Alone	100	1.40	0.60	1.99
Parallel surround	99	1.18	0.46	9.75
Orthogonal surround	100	1.15	0.53	3.20

Table 1. Contrast response function parameters. *Notes*: Parameters for Equation 1 were estimated by fitting the derivative to the average discrimination thresholds from four subjects presented in Figure 2.

round-Alone stimuli in a block design (12 s per block, eight Target-Alone and nine Surround-Alone blocks; total scan duration 3.2 min). This differential localizer approach was used in order to define a conservative target ROI (Olman et al., 2007). Disk and annulus stimuli matched the geometry used during task scans and were presented at 80% contrast. The task during these localizer scans was the same as in the Target-Alone and Surround-Alone conditions in the *Disks* experiments but with a 125-ms stimulus duration, 250-ms interstimulus interval, and 1.5-s trial onset interval.

The functional localizer for the *Gabors* experiments was a single-condition localizer with 12-s blocks of target Gabors at 80% pedestal contrast (same timing and task structure as above) alternating against 12-s blocks of target Gabors at 0% pedestal contrast ("blank" blocks).

Behavioral experiment

In order to estimate the magnitude of the orientation-dependent surround suppression for the *Disks* experiment, we investigated contrast discrimination performance in a subset of four subjects during a separate session inside the scanner using the concentric disk stimuli. Subjects performed the same 2IFC contrast discrimination task as in the *Attended Disks* experiment, using the same stimuli and presentation timing. Contrast discrimination thresholds for Target-Alone, Parallel, and Orthogonal conditions were measured at pedestal contrasts of 0% (detection), 1%, 2%, 4%, 8%, 16%, and 32%. When present, surrounds were displayed at 50% contrast. Thresholds were determined using a three-down, one-up staircase procedure. Thresholds were quantified by averaging the contrast increments presented in the last four trials for each condition in each run in which the staircases are expected to have converged at 79% accuracy (Garcia-Perez, 1998). Convergence was assessed by visual inspection of each subject's data, which confirmed that the staircases were stable at the end of each run. Threshold values were averaged across three runs per subject, each composed of 32 trials per condition. Contrast discrimination performance for a given pedestal contrast is assumed to be determined by the local derivative of the contrast

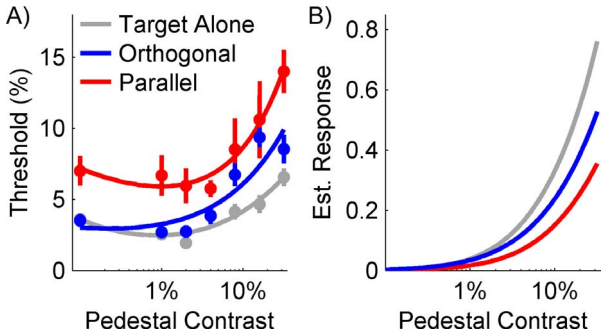

Figure 2. Psychophysics results. (A) Contrast discrimination thresholds for *Disks* stimuli. Error bars show *SEM* across subjects. Solid lines show fits to the derivative of the modified Naka-Rushton formula (Equation 1 and Table 1). (B) Estimated *Disks* contrast response functions. Responses are scaled relative to the maximum Target-Alone response at 100% contrast.

response function (Boynton et al., 1999; Legge & Foley, 1980; Yu et al., 2003), which we modeled as

$$R = \frac{AC^p}{C^{p-q} + \sigma^{p-q}} \quad (1)$$

R is the predicted response, and C is the pedestal contrast. The variable A scales the response magnitude whereas p, q, and σ describe the shape of the contrast response function. This function takes on an exponential shape set by p at low contrasts (below σ) and by q at higher contrasts. We estimated the contrast response for each observer by fitting the derivative of Equation 1 to the contrast discrimination threshold data from the Target-Alone, Parallel, and Orthogonal conditions using MATLAB's *lsqcurvefit*. Table 1 shows the parameters fit to the average threshold data from four subjects.

Psychophysical contrast discrimination thresholds (averaged across four subjects) for the *Disks* stimuli are shown in Figure 2A. Predicted contrast responses (Figure 2B) showed 30% suppression for parallel versus orthogonal surrounds across the range of pedestal contrasts used in our fMRI experiments (8%–32%).

Imaging data acquisition

FMRI data were collected at the University of Minnesota's Center for Magnetic Resonance Research on a Siemens 7 Tesla scanner equipped with the AC-84 head gradient insert, which has a maximum strength of 80 mT/m and a slew rate of 333 T/m/s. A custom-made radio frequency head coil (four-channel transmit, nine-channel receive; Adriany et al., 2012) was used for gradient echo (GE) echo-planar imaging (EPI). Images were acquired with a coronal field of view in 18 slices (1.2 mm thick) positioned near the occipital pole (Figure 3A). Image resolution was 1.2 mm isotropic;

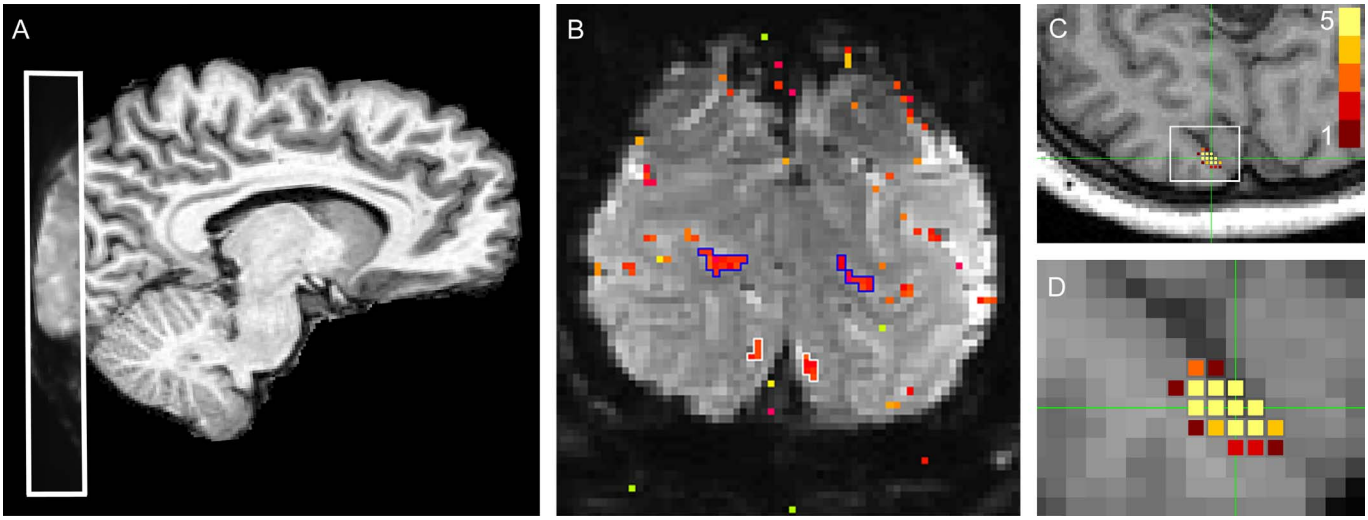

Figure 3. Functional coverage, EPI images and ROI localization. (A) Sagittal view of structural MRI with EPI data overlaid to show imaging coverage and alignment. Functional slice prescription outlined in white. (B) Representative functional data, single coronal slice in a single subject. Color overlay: voxels with coherence > 0.3 and peak response lag between 6–10 s (color indicates phase, with yellow being more delayed). V1 target ROIs (ventral, bilateral) are outlined in white, V2 target ROIs (dorsal, bilateral) in blue. (C) Axial view of structural MRI showing resampled positions for left ventral sub-ROI in V1 for five experiments in one subject. Voxels included in the sub-ROI are marked with colored squares. The color for each voxel indicates the number of experiments in which it was included in the sub-ROI (color bar at top right). Green crosshairs indicate the center of mass across experiments; white box indicates the region magnified in (D).

data were acquired with an in-plane parallel imaging acceleration factor (R) of two. Due to acoustic noise limitations following gradient maintenance, the following EPI acquisition parameters varied slightly between scanning sessions and are listed in Table 2: coverage, matrix size, echo time, echo spacing, and partial Fourier. The TR was 1.5 s. Task scans had 250 TRs in the *Disks*, *Attended Gabors*, and *Distracted Gabors* experiments and 264 TRs in the *Block Gabors* experiment, and functional localizer scans had 136 TRs in all experiments. Total scanning time in each experiment was approximately 1 hr.

Retinotopy

During a separate scanning session, a 1-mm isotropic T_1-weighted anatomical scan was acquired, and a retinotopic mapping experiment (Engel, Glover, & Wandell, 1997; Larsson & Heeger, 2006) was performed for each subject using standard rotating wedge and expanding ring checkerboard stimuli. Anatomical images were used to generate gray and white matter surface definition files (SurfRelax; Larsson, 2001). Occipital patches from inflated white matter surfaces were computationally flattened and used to visualize functional data when defining ROIs. The retinotopy data were used to functionally identify early visual areas (V1–3) with regional borders defined by phase reversals obtained in a correlational analysis.

Imaging data preprocessing

Imaging data were first converted from DICOM to NIFTI format (dinifti; http://cbi.nyu.edu/software/dinifti.php). Head motion was corrected using an iterative least-squares method (AFNI's 3dvolreg; Cox & Jesmanowicz, 1999). Geometric distortion compensation was conducted using a field map scan acquired during the EPI scanning session (FSL's FUGUE; S. M. Smith et al., 2004). Registration of the functional data to the T_1 anatomy (Nestares & Heeger, 2000) and ROI definition were completed using custom software in MATLAB.

Functional localization of target ROIs

Within retinotopically defined early visual areas (V1–3), ROIs were identified from the average of two functional localizer scans. Prior to analysis, the first eight frames of each localizer scan were discarded to ensure activation did not reflect artifacts related to scan onset. Functional localizer scans were then detrended by removing the first two Fourier components, and the two scans were then averaged. The Fourier transform of the average localizer time series was used to calculate

Experiment	# Subj.	FOV (mm)	Matrix size	TE (ms)	Echo spacing (ms)	Partial Fourier
Attended Disks	5	154 × 125	128 × 104	20	0.57	8/8
Attended Disks	4	154 × 135	128 × 112	20	0.70	7/8
Distracted Disks	10	154 × 135	128 × 112	20	0.70	7/8
Attended Gabors	5	154 × 154	128 × 128	18	0.52	7/8
Attended Gabors	4	154 × 135	128 × 112	20	0.70	7/8
Distracted Gabors	5	154 × 125	128 × 104	20	0.57	8/8
Distracted Gabors	4	154 × 135	128 × 112	20	0.70	7/8
Block Gabors	5	154 × 154	128 × 128	18	0.52	7/8
Block Gabors	4	154 × 135	128 × 112	20	0.70	7/8

Table 2. EPI scan parameters. *Notes*: For each experiment, the number of subjects (# Subj.) scanned with the listed parameters is noted in the second column. FOV = field of view (imaging coverage); TE = echo time.

the amplitude and phase of the response at the stimulus frequency (Engel et al., 1997). Coherence with stimulus presentation frequency was computed as the eight c/scan response amplitude divided by the square root of the time series power (this coherence is similar to an unsigned correlation coefficient). Activation was classified as significant above a threshold coherence level of 0.3. Phase values within a window of π to 1.6π (6- to 10-s peak response lag) were used to identify positive fMRI responses in phase with the target stimulus presentation (Figure 3B).

Within each visual area, ROIs consisting of up to four sub-ROIs were identified based on the location of significantly activated in-phase voxels. ROIs consisted of dorsal and ventral sub-ROIs in the left and right hemispheres, corresponding to the four target stimulus positions (one in each quadrant of the visual field). ROIs were then translated to the space of the in-plane functional images for manual refinement, which ensured that sub-ROIs consisted of a cluster of contiguous, significantly activated voxels (Figure 3B through D).

The average number of sub-ROIs within V1–3 and the number of voxels they contained is listed for all experiments in Table 3. It was not always possible to identify four separate in-plane sub-ROIs in all early visual areas for every subject. In particular, V3 sub-ROIs were identified least reliably. In some subjects, ventral sub-ROIs beyond V1 could not be identified due to insufficient imaging coverage in the anterior–posterior direction. As expected, the differential functional localizer for the *Disks* experiments produced smaller ROIs than the single-condition localizer used in the *Gabors* experiments. The restriction of ROI size by the differential localizer was most striking in V2 and V3 (compare the number of voxels between *Disks* and *Gabors* experiments in Table 3). This may be due to larger receptive field sizes in extrastriate areas (A. T. Smith, Singh, Williams, & Greenlee, 2001), which would be expected to yield large ROIs for a single-condition localizer but would limit the number of voxels that selectively respond to target but not surround stimuli in a differential localizer (Olman et al., 2007). Because of the small and inconsistent nature of the extrastriate ROIs in the *Disks* experiments, V2 and V3 ROIs in these two experiments were not analyzed further.

From published estimates of average cortical magnification factors in human visual cortex (Engel et al., 1997), we would expect a circular stimulus with a diameter of 1.5° presented at 3° eccentricity (as in the *Disks* experiments) to elicit an fMRI response across an approximately cylindrical region of V1, extending through the depth of the gray matter with a radius of roughly 4 mm. Note, however, that V1 surface area and cortical magnification can vary by as much as a factor of two between subjects (Duncan & Boynton, 2003). Assuming an average V1 cortical thickness of 2.5 mm, a 4-mm radius would predict a volume of activation of 126 mm^3 or about 73 voxels at 1.2 mm isotropic

	V1		V2		V3	
Experiment	# sub-ROIs	# voxels	# sub-ROIs	# voxels	# sub-ROIs	# voxels
Attended Disks	3.7 (0.5)	17 (10)	2.4 (1.1)	8 (11)	1.3 (0.7)	4 (3)
Distracted Disks	3.5 (0.7)	16 (13)	2.2 (1.3)	5 (13)	0.6 (0.8)	2 (1)
Attended Gabors	3.7 (0.7)	25 (15)	3.6 (0.7)	32 (17)	2.6 (0.9)	41 (40)
Distracted Gabors	3.8 (0.4)	31 (18)	3.6 (0.5)	43 (26)	2.8 (0.7)	48 (66)
Block Gabors	3.8 (0.4)	22 (7)	3.3 (0.7)	32 (16)	2.4 (0.5)	41 (38)

Table 3. Sub-ROI statistics. *Notes*: # sub-ROIs is the average across all subjects in each experiment. # voxels indicates the average number of voxels within each sub-ROI. Numbers in parentheses are standard deviation.

resolution. The average sub-ROI size in the *Disks* experiments was smaller than this, indicating that our differential localizer method was successful in identifying voxels that selectively responded to the target over the surround. Similarly, the target Gabor stimulus in the *Gabors* experiments (approximately 1° wide) would be expected to activate a 2.7-mm-radius cylindrical portion of V1 for an activation volume of 57 mm^3 or about 33 voxels. V1 sub-ROIs were smaller than this for the *Gabors* experiments on average, from which we conclude that our sub-ROI definition was conservative in these experiments as well, including only the most strongly modulated voxels representing the centers of the target Gabors.

Analysis of fMRI data

FMRI data from task scans were analyzed using a general linear model (GLM). AFNI's 3dDeconvolve (Cox, 1996) was used to estimate the fMRI response (percentage signal change from baseline) for each of the eight stimulus conditions in each voxel in each sub-ROI. Nuisance regressors were modeled using Legendre polynomials up to third order to remove temporal trends up to 1/150 s as well as the six motion parameters (roll; pitch; yaw; displacement in x, y, and z) estimated during motion correction. Volumes in which there was excessive motion (defined as a Euclidean norm of the temporal derivative for the six motion parameters above 0.3) were censored (excluded from the GLM analysis). For one subject who participated in all five experiments, a large proportion of volumes were censored (26% on average); this subject was one of the ones excluded, in this case from all experiments, due to unreliable data (see below). For all other subjects, an average of 2.4% ($SD = 1.5\%$) of volumes were censored or about six volumes per scan.

Response amplitude estimates were averaged across all voxels in all sub-ROIs for each visual area in each subject. For the event-related experiments, hemodynamic response functions (HRFs) were assessed separately for each subject and condition at 12 time points (18 s) following stimulus onset (i.e., response amplitudes were estimated using separate beta weights at each time point). Using a GLM to estimate the response at each time point avoids assumptions about HRF shape. The fMRI response amplitude was quantified as the average response between 3 and 4.5 s poststimulus (the peak response). The response baseline was defined using the signal measured during the first 6 s and final 15 s of each run, in which a mean gray screen was presented. For the *Block Gabors* experiment, individual HRFs were not estimated; instead, a canonical HRF (SPM; Friston et al., 1994) was used to model the BOLD response, and amplitude was estimated as the beta weight for each condition regressor with rest blocks used to define the response baseline.

A few subjects in each experiment showed particularly weak fMRI responses and noisy HRFs. In order to work with the most reliable data sets, we calculated the average t statistic for the estimated response amplitude within the V1 ROI across all eight stimulus conditions in each subject. In all experiments, data from one or two subjects were distinctly worse than the rest (e.g., HRFs that did not follow the canonical shape and average t statistics of 0.5 and 1.1 while remaining subjects' ranged from 1.6 to 2.9). In order to analyze the same amount of data in all experiments, we retained the seven subjects with the highest average t statistics in each experiment and excluded the rest (three subjects in *Distracted Disks*, two subjects in every other experiment). ROI sizes for the retained subjects were equivalent to those shown for all subjects in Table 3.

Responses were first analyzed simply in terms of percentage signal change to assess overall effects of experiment design and attention (see Results, "V1 fMRI responses"). Then, in order to facilitate comparisons between experiments, the Surround-Alone condition was used as a baseline for quantifying the response to the target stimulus. This analysis assumes that nonspecific responses to the surround within the target ROI are additive and thus can be accounted for by subtracting the Surround-Alone response. In essence, this assumes equal nonspecific surround responses regardless of the target contrast. Although it is likely that there is some small dependence of surround responses on the target, this selection of a baseline is consistent with previous studies (Millin et al., 2014; Pihlaja et al., 2008; Zenger-Landolt & Heeger, 2003).

Results

In five experiments, we examined how factors such as target contrast, surround orientation, stimulus geometry (*Disks* vs. *Gabors*), attention, hemodynamics, and experimental design (block vs. event-related) influenced the local fMRI response in visual cortex. The surround contrast was fixed at 50%. Targets were presented at lower contrast (0%–32%) than the surrounds in order to focus on surround suppression rather than facilitation (Shen et al., 2007; Xing & Heeger, 2001; Yu et al., 2001).

Functional MRI data from seven subjects were analyzed in each experiment. We used 1.2 mm GE EPI at 7 Tesla in order to achieve high spatial resolution imaging across early visual cortex with high BOLD contrast-to-noise ratio (Olman & Yacoub, 2011).

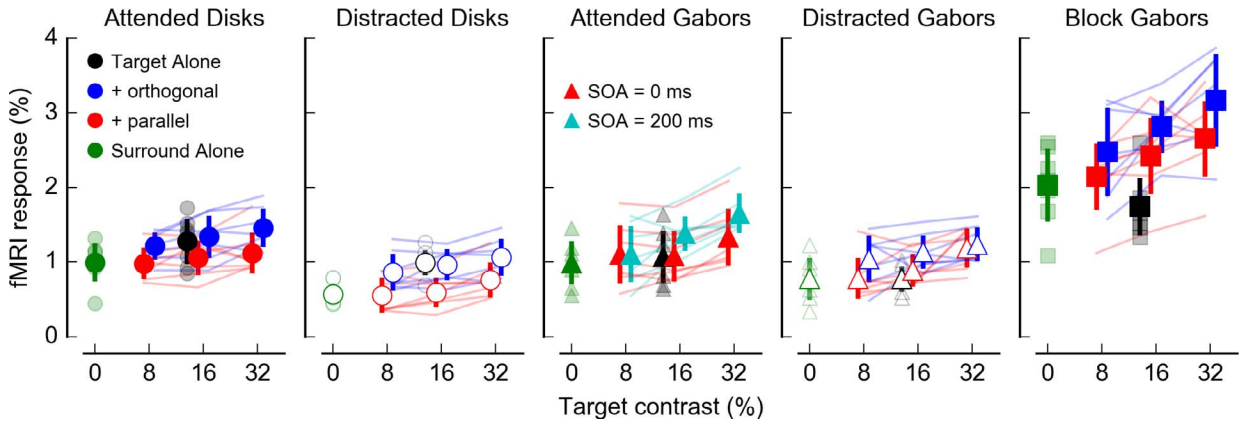

Figure 4. Responses in V1 ROIs for all experiments. Responses were calculated as percentage signal change relative to presentation of a mean gray screen. Pale lines and symbols indicate individual subject responses ($n = 7$). Symbol shape corresponds to stimulus geometry and presentation paradigm (indicated in titles). Open symbols indicate attention withdrawn from stimulus by a fixation task (see Methods, "*Distracted Disks* experiment"). Filled symbols indicate data acquired while subjects were engaged in a 2IFC contrast discrimination task, monitoring all four target locations for a contrast increment. Symbols are plotted with small offsets along the x-axis, here and in the following figures, to reduce overlap and improve visibility. Error bars indicate standard deviation.

Responses in small ROIs corresponding to the cortical representation of target stimuli in V1, V2, and V3 were measured while varying both the center target contrast and the surrounding stimulus configuration. We first report in detail the results in V1, then summarize findings in extrastriate cortex.

V1 fMRI responses

As expected (Huettel, Song, & McCarthy, 2009), the block-design experiment produced the largest fMRI responses in V1 (Figure 4, right panel). Also as expected (Buracas & Boynton, 2007; Li et al., 2008; Murray, 2008), attended stimuli (Figure 4, filled symbols) produced larger responses than unattended stimuli (open symbols). The average difference between fMRI responses for the *Attended* and *Distracted Disks* was 0.39% whereas the average difference for the *Gabors* was 0.24%. Results from an ANOVA testing the significance of different effects are tabulated in Table 4.

The data in Figure 4 show that responses to center and surround stimuli could not be fully separated. The *Disks* experiments used a differential localizer (see Methods, "Functional localization of target ROIs") to identify the cortical locations of the target stimuli, which maximizes selectivity of the resulting ROIs. However, the response to the Surround-Alone condition even in these conservative target ROIs was significantly greater than 0 (green symbols in Figure 4; Table 4.C.i). The *Gabors* experiments, on the other hand, used a single-condition localizer; this less conservative technique was selected for the *Gabors* experiments because the expected size of the cortical representations of the small stimuli was only ~5 mm in diameter on the cortical surface (see Methods, "Functional localization of target ROIs"), and a differential localizer would not have produced reliable ROI identification in all subjects. The poorer spatial selectivity of the single-condition localizer technique is evident in the fact that in the *Gabors* experiments (but not *Disks*), responses to targets presented alone at 16% contrast (Figure 4, black symbols) were not significantly larger than responses when surrounding stimuli were present without targets (Figure 4, green symbols and Table 4.C.iii). This means that responses to the surrounding context contributed just as much to the localized fMRI signals in the target ROIs as the targets themselves.

Because the target and surround responses were not fully separable even when using a differential localizer, further analyses of the effects of attention, surround orientation, and surround geometry on the fMRI responses to the target stimuli were performed after subtraction of the Surround-Alone response (see Methods and Discussion for caveats regarding this analysis decision). Target-Alone responses are therefore omitted from the following analyses because the use of the Surround-Alone condition as a baseline is not appropriate for that condition.

Baseline-subtracted V1 results

Results after Surround-Alone baseline subtraction are shown in Figure 5. The most striking result from this analysis is our observation that, in general, fMRI responses in V1 to targets with parallel surrounds were not significantly larger than the response to the

Analysis	Test	Statistic	Significance
A. Experiment	ANOVA main effect	$F(4, 30) = 31.2$	$p < 0.001$
i. Disks: Distracted < Attended	Post hoc *t* test	$t(110) = 6.91$	$p^{\dagger} < 0.001$
ii. Gabors*: Distracted < Attended	Post hoc paired *t* test	$t(34) = 3.76$	$p^{\dagger} < 0.001$
iii. Gabors*: Event-related < Block	Post hoc paired *t* test	$t(34) = 9.11$	$p < 0.001$
B. Condition	ANOVA main effect	$F(7, 30) = 50.6$	$p < 0.001$
C. Experiment × Condition	ANOVA interaction	$F(28, 210) = 6.12$	$p < 0.001$
i. All experiments: Surround-Alone > 0	Post hoc paired one-tailed *t*	$t(6) \geq 6.75$	$p^{\dagger} < 0.001$
ii. Disks: Surround-Alone < Target-Alone	Post hoc paired one-tailed *t*	$t(6) \geq 3.07$	$p^{\dagger} < 0.011$
iii. Gabors: Surround-Alone ≈ Target-Alone	Post hoc paired one-tailed *t*	$t(6) \leq 0.56$	$p^{\dagger} > 0.8$

Table 4. Statistical analyses of V1 fMRI responses. *Notes*: A two-way ANOVA compared response amplitudes from five experiments across eight conditions in seven subjects. All reported effects except the last were significant at $\alpha = 0.05$. False discovery rate (FDR) correction was used to adjust *p* values from post hoc tests for multiple comparisons. † FDR corrected for multiple comparisons. * 200-ms SOA and Orthogonal conditions were not compared due to stimulus differences.

Surround-Alone baseline (Table 5.G.i), and responses with orthogonal surrounds were robust (Table 5.G.ii). Overwhelming suppression by the parallel surrounding stimuli was not predicted from our psychophysical data (see Figure 2; Methods, "Behavioral experiment") but does agree with some electrophysiological studies in animals (Cavanaugh et al., 2002; Shen et al., 2007). Parallel responses in the *Block Gabors* experiment were an exception and tended to be larger than those obtained using the same stimuli in an event-related design, $t(20) = 2.08$, $p = 0.051$. Finally, in a control experiment, we observed that delaying the onset of parallel surrounds by 200 ms greatly reduced surround suppression for targets at 16% and 32% contrast (Table 5.B.ii and G.iii), indicating to what extent weak responses in the presence of parallel surrounds are the result of neural interactions rather than hemodynamic effects (Shmuel et al., 2002; A. T. Smith et al., 2004; Zenger-Landolt & Heeger, 2003).

Another salient feature of these data is that attention had no obvious effect on overall response amplitudes across experiments (Table 5.A). This indicates that subtracting the Surround-Alone response eliminated the effect of attention observed across experiments (Figure 4 and Table 4.A) and suggests that attention increased the response baseline for both target and surround stimuli (even though attention was directed at the targets in a 2IFC contrast-discrimination task).

In the absence of attention, the orientation-dependence of surround suppression (i.e., the difference between parallel and orthogonal surrounds) was stronger for the *Disks* geometry than for the *Gabors* geometry (Table 5.D.ii). This effect is expected because the ratio of surround to target area was 3:1 for the *Disks* geometry as opposed to 2:1 for the *Gabors*, although in the Discussion we will consider how the greater degree of surround contamination in the *Gabors* ROIs may confound this finding. For the *Disks* experiment, attention did not significantly affect the orientation-dependence of surround supression (Table 5.D.i). Not that in the *Gabors* experiment, the inclusion of the 200-ms SOA control meant that an analysis of the interaction between attention and orientation was not possible for this stimulus geometry.

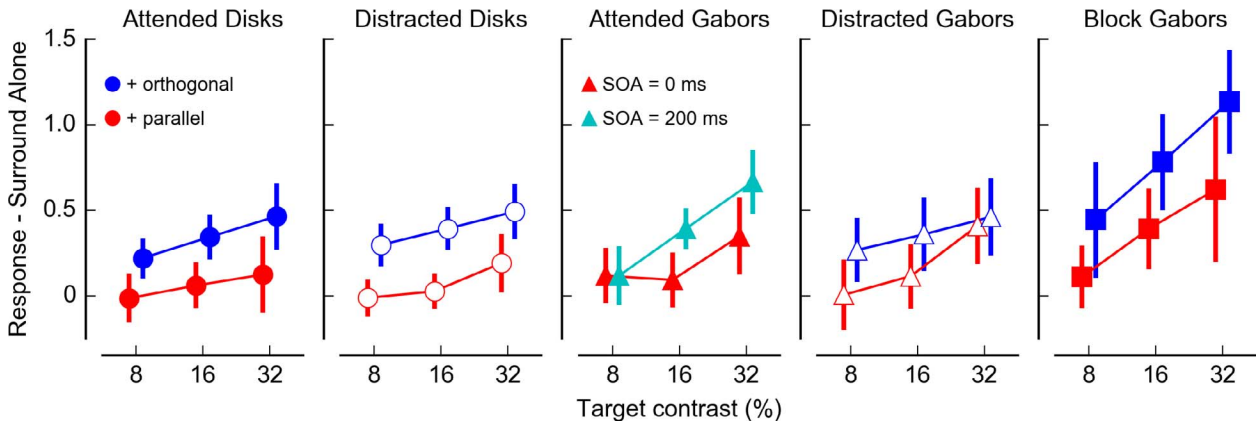

Figure 5. Target-present responses in V1 plotted relative to target-absent baseline to permit consideration of responses unique to target stimulus in spite of hemodynamic blurring. Error bars indicate standard deviation.

Analysis	Test	Statistic	Significance
A. Experiment	ANOVA main effect	$F(4, 30) = 1.17$	$p = 0.3$
B. Surround Configuration	**ANOVA main effect**	$\mathbf{F(1, 30) = 21.3}$	$\mathbf{p < 0.001}$
i. Block Gabors, Distracted Gabors, Attended Disks, Distracted Disks: Parallel < Orthogonal	**Post hoc paired *t* test**	$\mathbf{t(20) > 3.96}$	$\mathbf{p^{\dagger} < 0.001}$
ii. Attended Gabors: 0 ms < 200 ms SOA	**Post hoc paired *t* test**	$\mathbf{t(20) = 3.66}$	$\mathbf{p = 0.0016}$
C. Contrast	**ANOVA main effect**	$\mathbf{F(1, 30) = 123}$	$\mathbf{p < 0.001}$
D. Experiment × Surround	ANOVA interaction	$F(4, 30) = 1.71$	$p = 0.173$
i. Disks (Orthogonal–Parallel): Attended ≈ Distracted	Post hoc *t* test	$t(12) = 0.74$	$p^{\dagger} = 0.5$
ii. Distracted (Orthogonal–Parallel): Gabors < Disks	**Post hoc *t* test**	$\mathbf{t(12) = 4.24}$	$\mathbf{p^{\dagger} = 0.0023}$
E. Experiment × Contrast	**ANOVA interaction**	$\mathbf{F(4, 60) = 5.90}$	$\mathbf{p = 0.0013}$
F. Surround × Contrast	ANOVA interaction	$F(2, 60) = 1.36$	$p = 0.3$
G. Experiment × Surround × Contrast	*ANOVA interaction*	*F(4, 30) = 2.48*	*p = 0.065*
i. Parallel response > 0			
a. Distracted Gabors, 32%	**Post hoc paired one-tailed *t***	$\mathbf{t(6) = 4.49}$	$\mathbf{p^{\dagger} = 0.039}$
b. All other experiments and contrasts	Post hoc paired one-tailed *t*	$t(6) \leq 3.60$	$p^{\dagger} \geq 0.085$
ii. Orthogonal response > 0			
a. Block Gabors, 8%; Distracted Gabors, 8% and 16%	Post hoc paired one-tailed *t*	$t(6) \leq 4.10$	$p^{\dagger} \geq 0.057$
b. All other experiments and contrasts	**Post hoc paired one-tailed *t***	$\mathbf{t(6) \geq 4.54}$	$\mathbf{p^{\dagger} \leq 0.039}$
iii. 200 ms SOA response > 0			
a. Attended Gabors, 8%	Post hoc paired one-tailed *t*	$t(6) = 1.68$	$p^{\dagger} = 0.7$
b. Attended Gabors, 16% and 32%	**Post hoc paired one-tailed *t***	$\mathbf{t(6) \geq 7.93}$	$\mathbf{p^{\dagger} \leq 0.003}$

Table 5. Statistical results from an omnibus analysis of V1 fMRI responses (after subtracting Surround-Alone). *Notes*: A three-way ANOVA compared responses across five experiments, two surround configurations, and three target contrasts in seven subjects. Bold indicates a significant effect at $\alpha = 0.05$. Italics indicate a trend at $\alpha = 0.10$. † False discovery rate corrected for multiple comparisons.

Extrastriate cortex

Functional MRI responses were also measured in extrastriate areas V2 and V3. ROIs in V2 and V3 could not be reliably identified in the *Disks* experiments because the differential localizer produced such small regions of activation (see Methods, "Functional localization of target ROIs", and Table 3). Therefore, V2 and V3 fMRI responses were examined only in the *Gabors* experiments.

Larger responses were again evident with attention and for the blocked experimental design, as in V1 (Figure 6, top row). Isolation of target ROIs from surrounding regions was even worse in V2 and V3 than in V1, likely due to larger receptive fields in V2 and V3 (Burkhalter, Felleman, Newsome, & Van Essen, 1988; Gattass, Gross, & Sandell, 1981; A. T. Smith et al., 2001). This was evident in the fact that Target-Alone responses were not larger than Surround-Alone in V2 and V3 (Table 6.A.iii.a and B.iii.a). After subtracting out the Surround-Alone condition from V2 and V3 fMRI responses to targets with parallel and orthogonal surrounds (Figure 6, bottom row), we observed the expected ODSS and SOA-dependent suppression in V2 (Table 6.C.ii), but these effects were not significant in V3 (Table 6.D.ii). V2 and V3 responses showed weak sensitivity to target contrast in general with the exception of the 200-ms SOA condition in the *Attended Gabors* experiment.

Thus, the fMRI responses in V2 and V3 were qualitatively similar to responses in V1, which is very typical for fMRI studies of early visual responses to simplistic stimuli. With more complex (naturalistic or broadband) stimuli, an exciting study has recently shown unique sensitivity to higher order statistics in V2 that is absent in V1 (Freeman, Ziemba, Heeger, Simoncelli, & Movshon, 2013). But in these experiments, V2 and V3 responses did not differ greatly from those in V1.

Discussion

Using high-resolution fMRI at 7 Tesla, we have examined in detail the way in which manipulating target contrast, surround configuration, and the locus of attention may affect responses in early visual cortex. Our primary finding is that strong suppression of targets by parallel surrounding annuli or flanking Gabors renders responses to low-contrast (8% and 16%) stimuli essentially undetectable in event-related designs, and responses to the same targets are more robust with orthogonal surrounds or when presented in a blocked design. Although

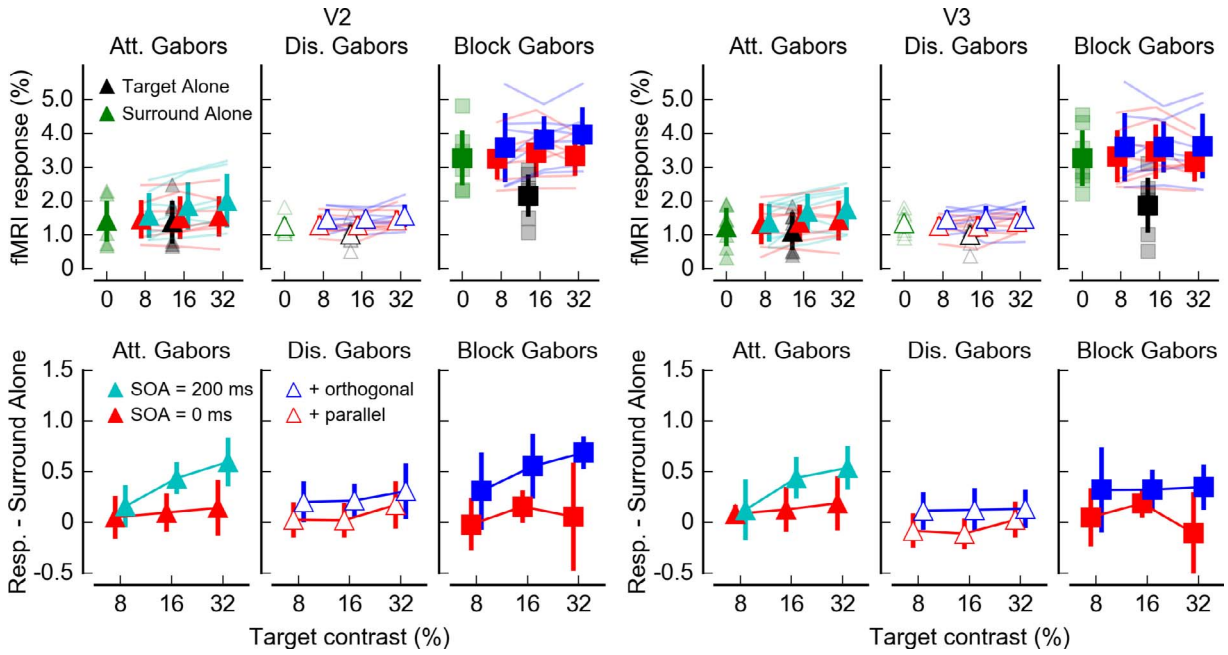

Figure 6. V2 and V3 results. Top row: fMRI responses. Bottom row: responses after subtraction of each subject's response to the Surround-Alone condition (units are still percentage signal change, but now relative to Surround-Alone condition). Colors and symbols as in previous figures.

directing attention to the stimuli caused a nonselective increase in response to all stimulus conditions, there was no obvious effect of attention after subtracting the response to the Surround-Alone. Below, we consider the implications for each aspect of this experiment (geometry, orientation, experiment design, and attention) in the context of existing literature and then discuss the impact of imaging resolution on studies of this nature.

Orientation dependence of suppression

Responses with parallel surrounds were dramatically lower than responses with orthogonal surrounds; most noticeable was the fact that the response at 8% contrast was essentially the same as the response at 0% (Surround-Alone) when surrounds were parallel. This suppression by parallel surround is much larger than predicted by psychophysical data for the *Disks* geometry, which estimated that the response to stimuli with parallel context should be reduced by 20%–40% relative to stimuli with orthogonal context. For the *Gabors* geometry, psychophysical data acquired as a part of a previous study (Schumacher & Olman, 2010) estimated that responses to targets with parallel context should be reduced by 10%–30% relative to the orthogonal conditions. Although our fMRI data agree qualitatively with these predictions—more response suppression for the *Disks* geometry than for the *Gabors*—they do not agree quantitatively. Attended stimuli with parallel contexts produced responses that were reduced by at least 50% relative to the orthogonal context for 16% contrast targets (Figure 5); the suppression was even greater for 8% contrast stimuli. Therefore, our estimates of fMRI response suppression by parallel context for attended stimuli are larger than predicted by psychophysics.

Nurminen et al. (2009) have also considered how methodological differences between fMRI and psychophysics may produce disparate estimates of surround suppression. As in the current study, they found that surround suppression in the V1 fMRI response was stronger than predicted from human psychophysics or macaque electrophysiology. These authors suggested that suppression may dominate the fMRI signal because fMRI reflects the summed response of many neurons with different feature preferences contained within a single voxel, a proposal that is supported by their modeling work. They posited that if suppression is more broadly tuned than excitation for features such as orientation (Cavanaugh et al., 2002; Webb et al., 2005), suppression across a neural population might be stronger than within the subpopulation measured in electrophysiology (and presumably sampled in psychophysics), whose feature preference matches the target stimulus.

A related argument rests on the widely held belief that fMRI best reflects network-level activity as measured by local field potentials (Logothetis, Pauls, Augath, Trinath, & Oeltermann, 2001; Maier et al.,

Analysis	Test	Statistic	Significance
A. fMRI responses in V2			
i. Experiment	**ANOVA main effect**	$\boldsymbol{F(2, 18) = 22.5}$	$\boldsymbol{p < 0.001}$
a. V2: Distracted < Attended*	*Post hoc paired t* test	$t(34) = 1.91$	$p^{\dagger} = 0.065$
b. V2*: Attended < Block	**Post hoc paired *t test***	$\boldsymbol{t(34) = 10.7}$	$\boldsymbol{p^{\dagger} < 0.001}$
ii. Condition	**ANOVA main effect**	$\boldsymbol{F(7, 18) = 41.7}$	$\boldsymbol{p < 0.001}$
iii. Experiment × Condition	**ANOVA interaction**	$\boldsymbol{F(14, 126) = 8.70}$	$\boldsymbol{p < 0.001}$
a. V2: Surround-Alone ≈ Target-Alone	Post hoc paired one-tailed *t*	$t(6) \leq -0.30$	$p^{\dagger} > 0.9$
B. fMRI responses in V3			
i. Experiment	**ANOVA main effect**	$\boldsymbol{F(2, 18) = 21.4}$	$\boldsymbol{p < 0.001}$
a. V3*: Distracted ≈ Attended	Post hoc paired *t* test	$t(34) = 0.51$	$p^{\dagger} = 0.6$
b. V3*: Attended < Block	**Post hoc paired *t* test**	$\boldsymbol{t(34) = 11.8}$	$\boldsymbol{p^{\dagger} < 0.001}$
ii. Condition	**ANOVA main effect**	$\boldsymbol{F(7, 18) = 32.2}$	$\boldsymbol{p < 0.001}$
iii. Experiment × Condition	**ANOVA interaction**	$\boldsymbol{F(14, 126) = 8.33}$	$\boldsymbol{p < 0.001}$
a. V3: Surround-Alone ≈ Target-Alone	Post hoc paired one-tailed *t*	$t(6) \leq -0.91$	$p^{\dagger} > 0.9$
C. V2 fMRI responses − Surround-Alone			
i. Experiment	ANOVA main effect	$F(2, 18) = 0.70$	$p = 0.9$
ii. Surround Configuration	*ANOVA main effect*	$F(1, 18) = 4.35$	$p = 0.051$
a. Block, Distracted: Para. < Orth.	**Post hoc *t* test**	$\boldsymbol{t(20) \geq 4.80}$	$\boldsymbol{p^{\dagger} < 0.001}$
b. Attended: 0 < 200 ms SOA	**Post hoc *t* test**	$\boldsymbol{t(20) = 4.35}$	$\boldsymbol{p < 0.001}$
iii. Contrast	**ANOVA main effect**	$\boldsymbol{F(1, 18) = 29.2}$	$\boldsymbol{p < 0.001}$
iv. Experiment × Surround	ANOVA interaction	$F(2, 18) = 0.49$	$p = 0.6$
v. Experiment × Contrast	ANOVA interaction	$F(2, 18) = 0.85$	$p = 0.4$
vi. Surround × Contrast	**ANOVA interaction**	$\boldsymbol{F(1, 18) = 6.82}$	$\boldsymbol{p = 0.018}$
vii. Experiment × Surround × Contrast	ANOVA interaction	$F(2, 18) = 2.56$	$p = 0.105$
D. V3 fMRI responses − Surround-Alone			
i. Experiment	**ANOVA main effect**	$\boldsymbol{F(2, 18) = 4.81}$	$\boldsymbol{p = 0.021}$
ii. Surround Configuration	ANOVA main effect	$F(1, 18) = 1.40$	$p = 0.3$
iii. Contrast	*ANOVA main effect*	$F(1, 18) = 4.15$	$p = 0.057$
iv. Experiment × Surround	ANOVA interaction	$F(2, 18) = 0.40$	$p = 0.7$
v. Experiment × Contrast	**ANOVA interaction**	$\boldsymbol{F(2, 18) = 6.28}$	$\boldsymbol{p = 0.0086}$
vi. Surround × Contrast	ANOVA interaction	$F(1, 18) = 1.39$	$p = 0.3$
vii. Experiment × Surround × Contrast	ANOVA interaction	$F(2, 18) = 1.14$	$p = 0.3$

Table 6. Statistical results from analyses of V2 and V3 fMRI responses to Gabor stimuli. *Notes*: Raw responses were compared in two-way ANOVAs across three experiments and eight stimulus conditions in seven subjects. After subtracting the response to the Surround-Alone, responses were examined in three-way ANOVAs across three experiments, two surround configurations, and three target contrasts in seven subjects. Bold indicates a significant effect at $\alpha = 0.05$. Italics indicate a trend at $\alpha = 0.10$. † False discovery rate corrected for multiple comparisons. * 200-ms SOA and Orthogonal conditions were not compared due to stimulus differences.

2008), whereas psychophysics may be more closely related to neural spiking. Surround suppression likely involves a simultaneous reduction in both excitation and inhibition (Ozeki, Finn, Schaffer, Miller, & Ferster, 2009; Rubin, Van Hooser, & Miller, 2015; Shushruth et al., 2012). Greater surround suppression of excitatory and inhibitory conductance (compared with spike rate suppression) has also been reported (Anderson, Lampl, Gillespie, & Ferster, 2001). These results may provide a reasonable framework for interpreting this discrepancy; greater suppression as observed by fMRI versus psychophysics (or electrophysiology) may reflect suppression throughout the local network, which is stronger than the suppression of action potentials in the subpopulation of neurons whose preferred orientation matches the target stimulus.

In the absence of single-unit recordings of contrast response functions for attended *Gabor* and *Disk* stimuli, there is no obvious way to determine whether the fMRI data do not provide a good match to the psychophysics because they reflect different neuronal signals or because fMRI does not adequately characterize the underlying neural response. Weighing in favor of the adequacy of the fMRI data is the fact that the contrast response functions for the *Distracted Disks* provide a reasonable match to reported electrophysiology data from anaesthetized animals (Cavanaugh et al., 2002; Shen et al., 2007). This is true despite the fact that electrophysiology experiments typically use stimuli matched to the feature

preferences of the neuron being recorded from, and our fMRI data likely reflect the responses of many non-optimally stimulated neurons. However, the overall fMRI baseline offset that results from attention (Buracas & Boynton, 2007; Li et al., 2008; Murray, 2008) as well as the potential for increasingly complex interactions between target and surround representations in the fMRI signal when the stimuli are attended (Flevaris & Murray, 2015), reflect how fMRI is sensitive to a diverse set of local neuronal signals. This diversity increases the challenge of obtaining quantitative estimates of response suppression for attended stimuli using fMRI.

Interaction of orientation and attention

Directing attention away from the peripheral gratings using a distracting fixation task had little effect on the difference between the parallel and orthogonal surround conditions for the *Disks* experiment. This result is in conflict with a previous report, which found stronger ODSS in a psychophysical task when subjects performed a divided attention task versus when attention was directed only to peripheral gratings (Zenger et al., 2000). This may be explained by the fact that in our paradigm subjects directed their attention *exclusively* to a central fixation task and were not told to divide their attention.

We also observed that attention increased the response to the Surround-Alone condition as much as to the conditions with target present; that is, responses to target stimuli, once the Surround-Alone baseline was subtracted, were no larger with attention than without. This finding certainly does not generalize to all studies of surround modulation of small image features. For example, Flevaris and Murray (2015) found very clear effects of focal attention when cuing subjects to attend to either targets or flankers. Several other studies have also demonstrated that, in complex visual environments, attention can be either focal or distributed (Gilbert, Ito, Kapadia, & Westheimer, 2000; Pestilli, Carrasco, Heeger, & Gardner, 2011; Sundberg, Mitchell, & Reynolds, 2009) with very different behavioral and electrophysiological results depending on the spatial scale of the attention field. Our task required subjects to monitor four locations in space at 3° eccentricity, which may have encouraged a broader attentional focus than a task directed at a single stimulus.

Block versus event-related design

Responses to *Attended Gabor* stimuli with parallel surrounds were more reliably detected in a block-design experiment than in an event-related design. There are three possibilities for this: (a) The block-design experiment produced less suppression, perhaps because the predictability of the blocked stimuli decreased center–surround interactions; (b) nonspecific hemodynamic responses to the surrounding stimuli masked the target responses and were stronger in the event-related condition; or (c) the increased contrast-to-noise ratio of the block design permitted reliable detection of very weak signals. Arguing against the first possibility is the fact that psychophysical data were acquired with both blocked (Figure 2) and randomized (data not shown) condition order, and both data sets make equivalent predictions: Parallel surrounds should produce at most 40% suppression compared to orthogonal surrounds. Thus, we found no behavioral evidence for a dependence of suppression magnitude on stimulus presentation paradigm (blocked vs. randomized).

Arguing against the second possibility (nonlinear contributions by surrounds are stronger in event-related design), we have two observations. First, contributions by surrounds to the target ROIs were stronger in the *Block Gabors* than in the *Attended Gabors* event-related experiment. Second, we performed a separate analysis (not shown) in which the data from each subject in each experiment were divided by the mean response to all eight conditions. This normalization removed overall amplitude differences between block and event-related designs and allowed more direct comparison between block and event-related designs. This analysis approach is not reported in the Results because it is not appropriate for comparing Distracted and Attended experiments; it artificially inflates differences between Parallel and Orthogonal responses in the Distracted experiments relative to Attended experiments because of the additive effect of attention on the fMRI response. This analysis showed that the responses were as large, on average and in proportion to the Surround-Alone baseline, in the event-related design as in the block design.

Therefore, we conclude in favor of the third possibility: The difference between block and event-related results is simply a matter of contrast-to-noise ratio. Although blocked designs lack a degree of ecological relevance, the improved efficiency appears valuable for quantifying very small effects of context on small image features.

Geometry

We observed a larger difference between Orthogonal and Parallel responses with the *Disks* versus the *Gabors* stimulus geometry, which may be expected given the ratio of stimulus sizes in each experiment (surround

was three times larger than the target in the *Disks* and two times larger for *Gabors*). Although this interpretation appears most straightforward and perhaps most parsimonious, there is another explanation that may also bear consideration. Equivalent suppression may not be evoked by all surround regions (Cavanaugh et al., 2002; Chen, 2014; Coen-Cagli, Dayan, & Schwartz, 2012; Walker et al., 1999), and for the *Gabors*, the surrounding stimuli flanked the target region (i.e., were not collinear; Figure 1) while the annular surrounds completely enclosed the *Disks*. Because collinear texture (as provided by the *Disks* surrounds) often provides facilitation (Cavanaugh et al., 2002; Levitt & Lund, 1997; Yu et al., 2001), it is possible that, in spite of increased size relative to the center size, the surrounds in the *Disks* experiments were not necessarily more suppressive than those in the *Gabors*. Instead, the greater contamination by surround signal in the *Gabors* ROIs could have created the appearance of a weaker effect of orientation. If target and surround responses do not sum linearly (as described in the Introduction) and this nonlinearity is stronger for ROIs in the *Gabors* experiment, then this might produce a smaller difference between Parallel and Orthogonal responses.

Do hemodynamic nonlinearities confound measurements of very small stimuli with fMRI?

This series of experiments confronts a fundamental limitation of fMRI: Because of the spatial overlap between cortical representations of center and surround regions, extraclassical surround suppression for adjacent small image elements cannot be directly measured with this technique. In invasive electrophysiology experiments, particularly those using anesthetized animals, it is possible to isolate signals from individual neurons that show no increase in firing rate when stimuli are presented in nearby regions of the extraclassical surround. In fMRI experiments, on the other hand, we are measuring populations of neurons that span at least the size of our voxels (1.2 mm in this case), and because of blurring due to subject motion and other image acquisition details (e.g., T_2^* blurring; Olman & Yacoub, 2011), the true resolution is worse than the nominal resolution. Therefore, nonzero responses to the surrounding textures will be measured in even the most conservative ROI because we are studying responses to stimuli with cortical representations that are only a few millimeters across.

Previous studies (e.g., the 3.3° annuli at 6° eccentricity used in Zenger-Landolt & Heeger, 2003) have addressed this problem by calculating suppression as the difference between two measurements. First, the target is presented (in an on/off block design) with no surround present; then (in a separate scan) the target is presented (again in an on/off block design) while the surround is always present, and the magnitude of the suppression is calculated as the difference between the target responses with and without surround. Our use of the Surround-Alone baseline for calculating contrast response functions with parallel and orthogonal surrounds is analogous to this practice. However, to continue the analogy, we should then be able to compute surround suppression at 16% contrast by comparing the amplitude of the Target-Alone condition (16% contrast) against the baseline-subtracted target + surround conditions to derive an estimate of surround suppression. In Figure 4, the typical Target-Alone (16% contrast, unsuppressed) response is a 1% signal change. In Figure 5, the typical response to a 16% contrast target with orthogonal surrounds is less than 0.5%. This comparison would estimate that the orthogonal surrounds are providing 50% suppression. However, for ~16% contrast targets with higher contrast orthogonal surrounds, the electrophysiology literature indicates suppression should be weaker than 50% (Cavanaugh et al., 2002; Levitt & Lund, 1997), and many cells show facilitation by orthogonal surrounds. Suppression magnitudes of 50% are typically only seen in the electrophysiology literature for parallel surrounds. Therefore, we conclude that residual hemodynamic nonlinearities are present and preclude estimation of the overall magnitude of surround suppression (center alone vs. center + surround) in the event-related design, and only relative comparisons (parallel vs. orthogonal) are valid.

Our third experiment, which used a SOA to reduce neuronal interactions between the *Attended Gabor* centers and surrounds, produced an estimate of the magnitude of the unsuppressed neural response to central targets (with SOA = 200 ms) that is better aligned with electrophysiological literature. That experiment estimates the unsuppressed target response to be about twice as large as the response to the (attended) target with simultaneously presented parallel surround. In the block-design experiment in which the Gabor stimuli were likewise attended, the response with orthogonal surrounds was also twice as large as the response with parallel surrounds. So, in combination, these two experiments indicate roughly 50% suppression for 16% contrast targets with parallel surrounds and very little suppression from orthogonal surrounds. Obviously, that logic is indirect, and the ideal comparison would include a sixth experiment to permit direct comparison between synchronous and asynchronous orthogonal surrounds, both with event-related designs. However, the indirect route suggests that our results in this case are consistent with the electrophysiological literature.

Still, we are left without an explanation for why the Target-Alone condition produced a ~1% modulation

from baseline while the presumably unsuppressed targets in the SOA = 200 ms condition produced only a ~0.5% modulation from baseline. One possibility is that the SOA did not fully remove neural interactions between targets and surrounds. However, this is not likely because previous studies have found little or no suppression by surrounds presented at such an asynchrony (200 ms; Ishikawa et al., 2006; Petrov & McKee, 2009). The most likely explanation is that responses to the surround stimuli, unavoidably mixed (because they originate from the same tissue) with responses to the target stimuli, limit the dynamic range of the localized fMRI signal. In even the most conservative ROIs (*Disks* experiments), the response to the Surround-Alone condition was only slightly smaller than the Target-Alone response. Direct comparison of the unsuppressed target responses (Target-Alone, black triangle, middle panel, Figure 4 vs. 200 ms SOA at 16% contrast, cyan triangle, middle panel, Figure 5) indicates ~50% amplitude reduction due to these apparently nonlinear hemodynamic effects of the surrounding stimuli.

Comparison against other measurements of surround suppression of small image features

When the stimuli in question have cortical representations that are comparable in size to the imaging resolution, using fMRI to measure surround suppression becomes difficult. Isolation of target and surround representations becomes more challenging, and our understanding of the heterogeneity of the underlying neuronal population (e.g., some populations of neurons are facilitated by orthogonal surrounds, and others are not) and the details of how attention is allocated to the task become more important. In this section, we discuss how our results are consistent with and extend other studies that have recently used fMRI to study surround suppression of isolated visual elements.

In 2010, our laboratory published a paper (Schumacher & Olman, 2010) showing that the measured response to the Gabor elements with parallel surrounds actually decreased as target contrast increased. With the results of the present study, we are now better able to understand the previous result. There are three contributing factors: isolation of the target response, suppression of flanking elements by targets, and locus of attention. The previous experiment was performed at 3 Tesla; the lower contrast-to-noise ratio of fMRI experiments at 3 Tesla, compared with 7 Tesla, meant that multiple experiments were required to estimate responses to all eight conditions in a single subject. Combining data across days degrades resolution, and the consequence for the previous experiment was even greater contamination of the target ROI by the surround responses than in the present study (which had higher imaging resolution, more conservative target ROI definitions, and within-session comparisons between conditions). Contamination of the target ROI by responses from the surround is not important if the surround responses are constant throughout the entire experiment, but there are two reasons that the surround responses may not be constant: (a) The targets provide surround suppression to the flankers and that effect will increase in strength as the target contrast increases, and (b) the strength with which the target responses suppress the surround responses may vary as a function of how selectively attention is allocated to the targets, and selective attention is easier the more dissimilar the features are (i.e., low-contrast targets or orthogonal surrounds). In the 2010 paper, we reported a control experiment in which subjects performed a contrast-discrimination task on the surrounding Gabors as target contrast was varied, and we saw no effect of the targets on the surrounds. However, in that psychophysical control experiment, attention was not directed at the targets, so their efficacy as a suppressive surround for the flanking Gabors may have been underestimated (Schwartz & Coen-Cagli, 2013). Therefore, it is likely that the portion of the signal in the target ROI that actually represents the surrounds (which is roughly 50% even with high spatial resolution) decreases as target contrast increases. Indeed, a simulation of these experiments conducted with an implementation of the flexible normalization model that also accounts for heterogeneity of responses across cortex (unpublished work) is able to replicate the findings of the 2010 paper when (a) surround responses dominate the ROI and (b) target stimuli provide suppression to the surrounds.

Recent studies from other groups have also highlighted the complex interactions between surround configuration, stimulus geometry, and the locus of attention, which must be considered when using fMRI to study the representation of small image features. Millin et al. (2014) used a method similar to ours to quantify the effect of crowding on the fMRI response to letter stimuli in early visual areas. They found no difference between responses to crowded targets versus flankers alone, and less crowded targets evoked larger responses. This was true regardless of whether attention was directed to the letters or toward a demanding fixation task. Their findings mirror the results we observed using grating stimuli, demonstrating that strong flanker suppression of small image features may be observed in a variety of fMRI paradigms. As noted above, Flevaris and Murray (2015) recently reported that the pattern of contextual modulation observed in the V1 fMRI response to a central target depends both on the orientation of flanking stimuli and on the locus

of attention. Using a normalization model, these authors showed that a combination of spatial- and feature-selective attention effects could account for a switch between iso-orientation surround suppression and surround enhancement when subjects shifted their attention between the target and flanking stimuli. McDonald, Mannion, Goddard, and Clifford (2010) have also shown how the response within a small target ROI may be contaminated by responses to surrounding stimuli (their figure 11), which may confound the interpretation of response differences between surround conditions. Together with the current study, this work highlights the need for careful experimental design and the role for predictive models in untangling complex interactions between stimulus context and behavioral task.

Keywords: surround suppression, functional MRI, attention, contextual modulation, contrast response function

Acknowledgments

We thank Cheng Qiu and Damien J. Mannion for scanning assistance, Stephan R. Brancel for help with data analysis, and the reviewers for their helpful comments. This work was supported by the National Science Foundation (GRF 00006595 to MPS), the National Institute of Health (R21 NS075525 to CAO, T32 GM00847, P30 EY011374, P30 NS076408, P41 EB015894, S10 RR026783), the University of Minnesota Graduate School (doctoral dissertation fellowship to MPS), and the WM KECK Foundation. The authors declare that they have no conflicts of interest, financial or otherwise.

Commercial relationships: none.
Corresponding author: Michael-Paul Schallmo.
Email: schal110@umn.edu.
Address: Graduate Program in Neuroscience, University of Minnesota, Minneapolis, MN, USA.

References

Adriany, G., Waks, M., Tramm, B., Schillak, S., Yacoub, E., DeMartino, F., . . .Ugurbil, K. (2012). An open faced 4 ch. loop transmit / 16 ch. receive array coil for HiRes fMRI at 7 Tesla. Paper presented at the 20th Annual Meeting of the International Society for Magnetic Resonance in Medicine, Melbourne, Australia.

Anderson, J. S., Lampl, I., Gillespie, D. C., & Ferster, D. (2001). Membrane potential and conductance changes underlying length tuning of cells in cat primary visual cortex. *The Journal of Neuroscience, 21*(6), 2104–2112.

Bao, P., Purington, C. J., & Tjan, B. S. (2015). Using an achiasmic human visual system to quantify the relationship between the fMRI BOLD signal and neural response. *eLife, 4*, e09600.

Bouvier, S. E., & Engel, S. A. (2011). Delayed effects of attention in visual cortex as measured with fMRI. *Neuroimage, 57*(3), 1177–1183.

Boynton, G. M., Demb, J. B., Glover, G. H., & Heeger, D. J. (1999). Neuronal basis of contrast discrimination. *Vision Research, 39*, 257–269.

Boynton, G. M., Engel, S. A., Glover, G. H., & Heeger, D. J. (1996). Linear systems analysis of functional magnetic resonance imaging in human V1. *Journal of Neuroscience, 16*(13), 4207–4221.

Brainard, D. (1997). The Psychophysics Toolbox. *Spatial Vision, 10*(4), 433–436.

Brefczynski, J. A., & DeYoe, E. A. (1999). A physiological correlate of the 'spotlight' of visual attention. *Nature Neuroscience, 2*(4), 370–374.

Bressler, D. W., Fortenbaugh, F. C., Robertson, L. C., & Silver, M. A. (2013). Visual spatial attention enhances the amplitude of positive and negative fMRI responses to visual stimulation in an eccentricity-dependent manner. *Vision Research, 85*, 104–112.

Buracas, G. T., & Boynton, G. M. (2007). The effect of spatial attention on contrast response functions in human visual cortex. *Journal of Neuroscience, 27*(1), 93–97.

Burkhalter, A., Felleman, D. J., Newsome, W. T., & Van Essen, D. C. (1988). Anatomical and physiological asymmetries related to visual areas V3 and VP in macaque extrastriate cortex. *Vision Research, 26*(1), 63–80.

Cannon, M. W., & Fullenkamp, S. C. (1991). Spatial interactions in apparent contrast: Inhibitory effects among grating patterns of different spatial frequencies, spatial positions and orientations. *Vision Research, 31*(11), 1985–1998.

Cavanaugh, J. R., Bair, W., & Movshon, J. A. (2002). Selectivity and spatial distribution of signals from the receptive field surround in macaque V1 neurons. *Journal of Neurophysiology, 88*, 2547–2556.

Chen, C.-C. (2014). Partitioning two components of BOLD activation suppression in flanker effects. *Frontiers in Neuroscience, 8*(149), 1–9.

Cheng, K., Wagooner, R. A., & Tanaka, K. (2001).

Human ocular dominance columns as revealed by high-field functional magnetic resonance imaging. *Neuron, 32*, 359–374.

Coen-Cagli, R., Dayan, P., & Schwartz, O. (2012). Cortical surround interactions and perceptual salience via natural scene statistics. *PLoS Computational Biology, 8*(3), e1002405.

Cox, R. W. (1996). AFNI: Software for analysis and visualization of functional magnetic resonance neuroimages. *Computers and Biomedical Research, 29*(3), 162–173.

Cox, R. W., & Jesmanowicz, A. (1999). Real-time 3D image registration for functional MRI. *Magnetic Resonance in Medicine, 42*, 1014–1018.

DeAngelis, G. C., Freeman, R., & Ohzawa, I. (1994). Length and width tuning of neurons in the cat's primary visual cortex. *Journal of Neurophysiology, 71*(1), 347–374.

Duncan, R. O., & Boynton, G. M. (2003). Cortical magnification within human primary visual cortex correlates with acuity thresholds. *Neuron, 38*(4), 659–671.

Engel, S. A., Glover, G. H., & Wandell, B. A. (1997). Retinotopic organization in human visual cortex and the spatial precision of functional MRI. *Cerebral Cortex, 7*(2), 181–192.

Flevaris, A. V., & Murray, S. O. (2015). Attention determines contextual enhancement versus suppression in human primary visual cortex. *The Journal of Neuroscience, 35*(35), 12273–12280.

Freeman, J., Ziemba, C. M., Heeger, D. J., Simoncelli, E. P., & Movshon, J. A. (2013). A functional and perceptual signature of the second visual area in primates. *Nature Neuroscience, 16*(7), 974–981.

Friston, K. J., Holmes, A. P., Worsley, K. J., Poline, J.-P., Frith, C. D., & Frackowiak, R. S. J. (1994). Statistical parametric maps in functional imaging: A general linear approach. *Human Brain Mapping, 2*, 189–210.

Garcia-Perez, M. A. (1998). Forced-choice staircases with fixed step sizes: Asymptotic and small-sample properties. *Vision Research, 38*(12), 1861–1881.

Gattass, R., Gross, C. G., & Sandell, J. H. (1981). Visual topography of V2 in the macaque. *The Journal of Comparative Neurology, 201*, 519–539.

Gilbert, C. D., Ito, M., Kapadia, M. K., & Westheimer, G. (2000). Interactions between attention, context and learning in primary visual cortex. *Vision Research, 40*, 1217–1226.

Heeger, D. J., Huk, A. C., Geisler, W. S., & Albrecht, D. G. (2000). Spikes versus BOLD: What does neuroimaging tell us about neuronal activity? *Nature Neuroscience, 3*(7), 631–633.

Henry, C. A., Joshi, S., Xing, D., Shapley, R. M., & Hawken, M. J. (2013). Functional characterization of the extraclassical receptive field in macaque V1: Contrast, orientation, and temporal dynamics. *The Journal of Neuroscience, 33*(14), 6230–6242.

Huettel, S. A., Song, A. W., & McCarthy, G. (2009). *Functional magnetic resonance imaging*. Sunderland, MA: Sinauer Associates, Inc.

Ishikawa, A., Shimegi, S., & Sato, H. (2006). Metacontrast masking suggests interaction between visual pathways with different spatial and temporal properties. *Vision Research, 46*(13), 2130–2138.

Joo, S. J., Boynton, G. M., & Murray, S. O. (2012). Long-range, pattern-dependent contextual effects in early human visual cortex. *Current Biology, 22*(9), 781–786.

Kastner, S., de Weerd, P., Desimone, R., & Ungerleider, L. G. (1988, Oct 2). Mechanisms of directed attention in the human extrastriate cortex as revealed by functional MRI. *Science, 282*, 108–111.

Kok, P., Bains, L. J., van Mourik, T., Norris, D. G., & de Lange, F. P. (2016). Selective activation of the deep layers of the human primary visual cortex by top-down feedback. *Current Biology, 26*(3), 371–376.

Kok, P., & de Lange, F. P. (2014). Shape perception simultaneously up- and downregulates neural activity in the primary visual cortex. *Current Biology, 24*, 1531–1535.

Larsson, J. (2001). *Imaging vision: Functional mapping of intermediate visual processes in man*. Stockholm, Sweden: Karolinska Institutet.

Larsson, J., & Heeger, D. J. (2006). Two retinotopic visual areas in human lateral occipital cortex. *The Journal of Neuroscience, 26*(51), 13128–13142.

Legge, G. E., & Foley, J. M. (1980). Contrast masking in human vision. *Journal of the Optical Society of America A, 70*(12), 1458–1471.

Levitt, J. B., & Lund, J. S. (1997, May 1). Contrast dependence of contextual effects in primate visual cortex. *Nature, 387*(6628), 73–76.

Li, X., Lu, Z.-L., Tjan, B. S., Dosher, B. A., & Chu, W. (2008). Blood oxygenation level-dependent contrast response functions identify mechanisms of covert attention in early visual areas. *Proceedings of the National Academy of Sciences, USA, 105*(16), 6202–6207.

Logothetis, N. K., Pauls, J., Augath, M., Trinath, T., & Oeltermann, A. (2001, July 12). Neurophysiological

investigation of the basis of the fMRI signal. *Nature*, *412*(6843), 150–157.

Maier, A., Wilke, M., Aura, C., Zhu, C., Ye, F. Q., & Leopold, D. A. (2008). Divergence of fMRI and neural signals in V1 during perceptual suppression in the awake monkey. *Nature Neuroscience, 11*(10), 1193–1200.

Malonek, D., & Grinvald, A. (1996, Apr 26). Interactions between electrical activity and cortical microcirculation revealed by imaging spectroscopy: Implications for functional brain mapping. *Science, 272*(5261), 551–554.

McDonald, J. S., Mannion, D. J., Goddard, E., & Clifford, C. W. G. (2010). Orientation-selective chromatic mechanisms in human visual cortex. *Journal of Vision, 10*(12):34, 1–12, doi:10.1167/10.12.34. [PubMed] [Article]

McDonald, J. S., Seymore, K. J., Schira, M. M., Spehar, B., & Clifford, C. W. G. (2009). Orientation-specific contextual modulation of the fMRI BOLD response to luminance and chromatic gratings in human visual cortex. *Vision Research, 49*(11), 1397–1405.

Millin, R., Arman, A. C., Chung, S. T. L., & Tjan, B. S. (2014). Visual crowding in V1. *Cerebral Cortex, 24*, 3107–3115.

Müller, N. G., & Kleinschmidt, A. (2004). The attentional 'spotlight's' penumbra: Center-surround modulation in striate cortex. *Neuroreport, 15*(6), 977–980.

Murray, S. O. (2008). The effects of spatial attention in early human visual cortex are stimulus independent. *Journal of Vision, 8*(10), 2, 1–11, doi:10.1167/8.10.2. [PubMed] [Article]

Nestares, O., & Heeger, D. J. (2000). Robust multiresolution alignment of MRI brain volumes. *Magnetic Resonance in Medicine, 43*(5), 705–715.

Nurminen, L., Kilpelainen, M., Laurinen, P., & Vanni, S. (2009). Area summation in human visual system: Psychophysics, fMRI, and modeling. *Journal of Neurophysiology, 102*, 2900–2909.

Nurminen, L., Kilpelainen, M., & Vanni, S. (2013). Fovea-periphery axis symmetry of surround modulation in the human visual cortex. *PLoS One, 8*(2), e57906.

Olman, C. A., Harel, N., Feinberg, D. A., He, S., Zhang, P., Ugurbil, K., & Yacoub, E. (2012). Layer-specific fMRI reflects different neuronal computations at different depths in human V1. *PLoS One, 7*(3), e32536.

Olman, C. A., Inati, S., & Heeger, D. J. (2007). The effect of large veins on spatial localization with GE BOLD at 3 T: Displacement, not blurring. *NeuroImage, 34*, 1126–1135.

Olman, C. A., Ugurbil, K., Schrater, P., & Kersten, D. (2004). BOLD fMRI and psychophysical measurements of contrast response to broadband images. *Vision Research, 44*(7), 669–683.

Olman, C. A., & Yacoub, E. (2011). High-field fMRI for human applications: An overview of spatial resolution and signal specificity. *The Open Neuroimaging Journal, 5*, 74–89.

Ozeki, H., Finn, I. M., Schaffer, E. S., Miller, K. D., & Ferster, D. (2009). Inhibitory stabilization of the cortical network underlies visual surround suppression. *Neuron, 62*, 578–592.

Pelli, D. (1997). The VideoToolbox software for visual psychophysics: Transforming numbers into movies. *Spatial Vision, 10*(4), 437–442.

Pestilli, F., Carrasco, M., Heeger, D. J., & Gardner, J. L. (2011). Attentional enhancement via selection and pooling of early sensory responses in human visual cortex. *Neuron, 72*(5), 832–846.

Petrov, Y., & McKee, S. P. (2006). The effect of spatial configuration on surround suppression of contrast sensitivity. *Journal of Vision, 6*(3):4, 224–238, doi:10.1167/6.3.4. [PubMed] [Article]

Petrov, Y., & McKee, S. P. (2009). The time course of contrast masking reveals two distinct mechanisms of human surround suppression. *Journal of Vision, 9*(1), 21, 1–11, doi:10.1167/9.1.21. [PubMed] [Article]

Pihlaja, M., Henriksson, L., James, A. C., & Vanni, S. (2008). Quantitative multifocal fMRI shows active suppression in human V1. *Human Brain Mapping, 29*, 1001–1014.

Pooresmaeili, A., Poort, J., Thiele, A., & Roelfsema, P. R. (2010). Separable codes for attention and luminance contrast in the primary visual cortex. *Journal of Neuroscience, 30*(38), 12701–12711.

Rubin, D. B., Van Hooser, S. D., & Miller, K. D. (2015). The stabilized supralinear network: A unifying circuit motif underlying multi-input integration in sensory cortex. *Neuron, 85*(2), 402–417.

Sanayei, M., Herrero, J. L., Distler, C., & Thiele, A. (2015). Attention and normalization circuits in macaque V1. *European Journal of Neuroscience, 41*(7), 949–964.

Schallmo, M.-P., & Murray, S. O. (2016). Identifying separate components of surround suppression. *Journal of Vision, 16*(1), 2, 1–12, doi:10.1167/16.1.2. [PubMed] [Article]

Schumacher, J. F., & Olman, C. A. (2010). High-resolution BOLD fMRI measurements of local

orientation-dependent contextual modulation show a mismatch between predicted V1 output and local BOLD response. *Vision Research, 50*(13), 1214–1224.

Schumacher, J. F., Thompson, S. K., & Olman, C. A. (2011). Contrast response functions for single Gabor patches: ROI-based analysis over-represents low-contrast patches for GE BOLD. *Frontiers in Systems Neuroscience, 5*(19), 1–10.

Schwartz, O., & Coen-Cagli, R. (2013). Visual attention and flexible normalization pools. *Journal of Vision, 13*(1):25, 1–24, doi:10.1167/13.1.25. [PubMed] [Article]

Shen, Z.-M., Xu, W.-F., & Li, C.-Y. (2007). Cue-invariant detection of centre-surround discontinuity by V1 neurons in awake macaque monkey. *Journal of Physiology, 583*(2), 581–592.

Shmuel, A., Yacoub, E., Pfeuffer, J., Van de Moortele, P.-F., Adriany, G., Hu, X., & Ugurbil, K. (2002). Sustained negative BOLD, blood flow and oxygen consumption response and its coupling to the positive response in the human brain. *Neuron, 36*(6), 1195–1210.

Shushruth, S., Mangapathy, P., Ichida, J. M., Bressloff, P. C., Schwabe, L., & Angelucci, A. (2012). Strong recurrent networks compute the orientation tuning of surround modulation in the primate primary visual cortex. *Journal of Neuroscience, 32*(1), 308–321.

Shushruth, S., Nurminen, L., Bijanzadeh, M., Ichida, J. M., Vanni, S., & Angelucci, A. (2013). Different orientation tuning of near- and far-surround suppression in macaque primary visual cortex mirrors their tuning in human perception. *The Journal of Neuroscience, 33*(1), 106–119.

Smith, A. T., Singh, K. D., Williams, A. L., & Greenlee, M. W. (2001). Estimating receptive field size from fMRI data in human striate and extrastriate visual cortex. *Cerebral Cortex, 11*(12), 1182–1190.

Smith, A. T., Williams, A. L., & Singh, K. D. (2004). Negative BOLD in the visual cortex: Evidence against blood stealing. *Human Brain Mapping, 21*(4), 213–220.

Smith, S. M., Jenkinson, M., Woolrich, M. W., Beckmann, C. F., Behrens, T. E. J., Johansen-Berg, H., . . .Matthews, P. M. (2004). Advances in functional and structural MR image analysis and implementation as FSL. *NeuroImage, 23*(S1), 208–219.

Snowden, R. J., & Hammett, S. T. (1998). The effects of surround contrast on contrast thresholds, perceived contrast, and contrast discrimination. *Vision Research, 38*, 1935–1945.

Sundberg, K. A., Mitchell, J. F., & Reynolds, J. H. (2009). Spatial attention modulates center-surround interactions in macaque area V4. *Neuron, 61*(6), 952–963.

Tadin, D., Lappin, J. S., Gilroy, L. A., & Blake, R. (2003, July 17). Perceptual consequences of centre–surround antagonism in visual motion processing. *Nature, 424*, 312–315.

Tootell, R. B. H., Hadjikhani, N. K., Vanduffel, W., Liu, A. K., Mendola, J. D., Sereno, M. I. & Dale, A. M. (1998). Functional analysis of primary visual cortex (V1) in humans. *Proceedings of the National Academy of Sciences, USA, 95*(3), 811–817.

Walker, G. A., Ohzawa, I., & Freeman, R. (1999). Asymmetric suppression outside the classical receptive field of the visual cortex. *Journal of Neuroscience*, *19*(23), 10536–10553.

Webb, B. S., Dhruv, N. T., Solomon, S. G., Tailby, C., & Lennie, P. (2005). Early and late mechanisms of surround suppression in striate cortex of macaque. *Journal of Neuroscience*, *25*(50), 11666–11675.

Williams, A. L., Singh, K. D., & Smith, A. T. (2003). Surround modulation measured with functional MRI in the human visual cortex. *Journal of Neurophysiology*, *89*, 525–533.

Xing, J., & Heeger, D. J. (2000). Center-surround interactions in foveal and peripheral vision. *Vision Research*, *40*, 3065–3072.

Xing, J., & Heeger, D. J. (2001). Measurement and modeling of center-surround suppression and enhancement. *Vision Research*, *41*(5), 571–583.

Yacoub, E., Harel, N., & Ugurbil, K. (2008). High-field fMRI unveils orientation columns in humans. *Proceedings of the National Academy of Sciences, USA*, *105*(30), 10607–10612.

Yu, C., Klein, S. A., & Levi, D. M. (2001). Surround modulation of perceived contrast and the role of brightness induction. *Journal of Vision*, *1*(1):3, 18–31, doi:10.1167/1.1.3. [PubMed] [Article]

Yu, C., Klein, S. A., & Levi, D. M. (2003). Cross-and iso-oriented surrounds modulate the contrast response function: The effect of surround contrast. *Journal of Vision*, *3*(8):1, 527–540, doi:10.1167/3.8.1. [PubMed] [Article]

Zenger, B., Braun, J., & Koch, C. (2000). Attentional effects on contrast detection in the presence of surround masks. *Vision Research, 40*(27), 3717–3724.

Zenger-Landolt, B., & Heeger, D. J. (2003). Response suppression in V1 agrees with psychophysics of surround masking. *The Journal of Neuroscience, 23*(17), 6884–6893.